FEMS Microbiology Ecology, 93, 2017, fix086

doi: 10.1093/femsec/fix086
Advance Access Publication Date: 7 July 2017
Research Article

RESEARCH ARTICLE

Actinobacteria phylogenomics, selective isolation from an iron oligotrophic environment and siderophore functional characterization, unveil new desferrioxamine traits

Pablo Cruz-Morales[1,†], Hilda E. Ramos-Aboites[1], Cuauhtémoc Licona-Cassani[1,‡], Nelly Selem-Mójica[1], Paulina M. Mejía-Ponce[1], Valeria Souza-Saldívar[2] and Francisco Barona-Gómez[1,*]

[1]Evolution of Metabolic Diversity Laboratory, Unidad de Genómica Avanzada (Langebio), Cinvestav-IPN, 36821 Irapuato, México and [2]Departamento de Ecología Evolutiva, Instituto de Ecología, Universidad Nacional Autónoma de México, Coyoacán, 04510 Ciudad de México, México

*Corresponding author: Evolution of Metabolic Diversity Laboratory, Unidad de Genómica Avanzada (Langebio), Cinvestav-IPN, 36821 Irapuato, México. Tel: +52 (462) 166-3017; E-mail: francisco.barona@cinvestav.mx
†Present address: The Australian Institute of Bioengineering and Nanotechnology, The University of Queensland. Brisbane, Australia.
‡Present address: Centro de biotecnología FEMSA, Instituto Tecnologico y de Estudios Superiores de Monterrey, Monterrey, Mexico
One sentence summary: Evolutionary patterns of desferrioxamine genes involved in biosynthesis and transport help to understand the chemical diversity of siderophores and bacterial adaptation.
Editor: Tillmann Lueders

ABSTRACT

Desferrioxamines are hydroxamate siderophores widely conserved in both aquatic and soil-dwelling Actinobacteria. While the genetic and enzymatic bases of siderophore biosynthesis and their transport in model families of this phylum are well understood, evolutionary studies are lacking. Here, we perform a comprehensive desferrioxamine-centric (*des* genes) phylogenomic analysis, which includes the genomes of six novel strains isolated from an iron and phosphorous depleted oasis in the Chihuahuan desert of Mexico. Our analyses reveal previously unnoticed desferrioxamine evolutionary patterns, involving both biosynthetic and transport genes, likely to be related to desferrioxamines chemical diversity. The identified patterns were used to postulate experimentally testable hypotheses after phenotypic characterization, including profiling of siderophores production and growth stimulation of co-cultures under iron deficiency. Based in our results, we propose a novel *des* gene, which we term *desG*, as responsible for incorporation of phenylacetyl moieties during biosynthesis of previously reported arylated desferrioxamines. Moreover, a genomic-based classification of the siderophore-binding proteins responsible for specific and generalist siderophore assimilation is postulated. This report provides a much-needed evolutionary framework, with specific insights supported by experimental data, to direct the future ecological and functional analysis of desferrioxamines in the environment.

Keywords: siderophores; desferrioxamine; Actinobacteria; phylogenomics; Cuatro Cienegas Basin

Received: 17 February 2017; **Accepted:** 4 July 2017

INTRODUCTION

Iron comprises up to 32% of the Earth's crust and plays an important role in the metabolism of all living organisms (Sheftel, Mason and Ponka 2012). Despite being highly abundant in its ferric form (Fe^{3+}), after the oxidation event that occurred in the Planet during the Precambrian, iron bioavailability became limited due to its poor and uneven distribution in its soluble form, ferrous iron (Fe^{2+}). As a consequence, metabolism of sessile organisms has evolved to the synthesis of siderophores, i.e. specialized Fe^{3+} scavenger metabolites, which allow bacteria, fungi and plants to assimilate iron needed as a nutrient (Hider and Kong 2010). A canonical example of this class of specialized metabolites are the hydroxamate siderophores called desferrioxamines (DFOs), mainly produced by genera belonging to the phylum Actinobacteria (Wang *et al.* 2014), but also by other unrelated families belonging to distantly related bacterial phyla, such as the Gammaproteobacteria (Essén, Johnsson and Bylund 2007) and Alphaproteobacteria (Smits and Duffy 2011).

In the soil-dwelling and aquatic model genus *Streptomyces*, which belongs to the Actinobacteria, the biosynthesis, regulation and transport of hydroxamate siderophores are relatively well documented (Barona-Gómez *et al.* 2006; Bunet *et al.* 2006; Tunca *et al.* 2007, 2009; Patel, Song and Challis 2010; Tierrafría *et al.* 2011). It is well established that *Streptomyces* and related species produce different hydroxamate siderophores through divergent biosynthetic gene clusters (BGC) involving non-ribosomal peptide synthetases (or NRPS), e.g. coelichelin (Lautru *et al.* 2005), and NRPS-independent peptide synthetases (or NIS). Amongst these, the most commonly produced DFOs by *Streptomyces* are the cyclic and the acyl-capped linear forms, DFO-E and DFO-B, respectively (Barona-Gómez *et al.* 2004, 2006; Yamanaka *et al.* 2005). Moreover, some interactions between model bacterial strains mediated by these specialized metabolites have been characterized (Traxler *et al.* 2012, 2013; Arias *et al.* 2015; Galet *et al.* 2015). Thus, *Streptomyces* and related genera are a suitable biological model for studying the evolution of DFOs, which may be useful for directing ecological and functional studies.

DFO biosynthesis and transport also have important physiological and morphological implications in *Streptomyces*. Biosynthesis of these siderophores is co-regulated by both iron and the preferred carbon source of this genus, *N*-acetylglucosamine (Craig *et al.* 2012). It has also been shown that under laboratory conditions, *Amycolatopsis* sp. AA4, a *Streptomyces* closely related species that produces the catechol-peptide siderophore amychelin, can sequester DFO-E produced by *Streptomyces coelicolor*, arresting production of amychelin and driving morphological changes through the pleiotropic regulator *bldN* (Traxler *et al.* 2012; Lambert, Traxler and Craig 2014). In agreement with this, it has been shown that mutation of *desE*, coding for the periplasmic siderophore-binding protein (SBP) acting as the main DFO receptor in *S. coelicolor*, specifically sensing DFO-E, impairs the development of this microorganism (Tierrafría *et al.* 2011).

Despite that SBPs show different degrees of specificity and represent the interface between the bacteria and the environment during siderophore-mediated iron assimilation, they have been overlooked by ecological studies. In *S. coelicolor*, CchF is the SBP encoded by the coelichelin or *cch* BGC (Lautru *et al.* 2005), and it has been implicated with specific transport of ferricoelichelin (Barona-Gómez *et al.* 2006; Patel, Song and Challis 2010). In contrast, CdtB, a BGC-independent transporter, has been shown to be capable of transporting DFO-B and ferricoelichelin (Bunet *et al.* 2006; Tierrafría *et al.* 2011), whereas DesE, the SBP coded by the DFO or *des* cluster, specifically transports DFO-E plus all linear DFOs, as well as other hydroxamate siderophores not produced by *Streptomyces* (Barona-Gomez *et al.* 2006; Patel, Song and Challis 2010; Tierrafría *et al.* 2011; Arias *et al.* 2015). All together, these results suggest that DFOs act at different levels within the cell, implying complex environmental dynamics involving nutritional and developmental traits.

Studies on the chemical ecology of DFOs so far have been limited to analysis of interspecies interactions under laboratory conditions (Yamanaka *et al.* 2005; Traxler *et al.* 2012, 2013; Galet *et al.* 2015). Nevertheless, such laboratory-based microbiological challenges using model bacterial organisms, at least in one case, have led to DFOs structural diversification (Traxler *et al.* 2013). Interestingly, in a different study, the same DFOs were shown to promote bacterial growth of non-siderophore-producing organisms, allowing isolation from aquatic environments of otherwise non-cultivable bacteria (D'onofrio, Crawford and Stewart 2010). The latter study reported the chemical structures of atypical phenylacetyl-substituted DFO variants produced by aquatic members of the genus *Micrococcus*. As this chemical modification has a drastic effect on the solubility of the resulting DFOs (Lewis *et al.* 2010), and this genus belongs to the early diverging family Micrococcaceae, a link between these chemical modifications with an early taxonomic affiliation may have a bearing in the ecology of DFOs.

In this study, we contribute to the understanding of siderophores evolution by looking at the natural history of the biological components supporting the vital function of siderophore-mediated bacterial iron assimilation, with a focus on DFOs. We reconstructed the evolutionary history of all *des* biosynthetic and transport genes, with an emphasis in the phylum Actinobacteria. Comprehensive phylogenomics lead to testable hypotheses that were experimentally investigated, implicating a novel gene (termed *desG*) in the biosynthesis of arylated DFOs in *Micrococcus* and *Streptomyces*; as well as a genome-wide evolutionary classification for SBPs with functional and ecological implications. We linked this evolutionary analysis to the environment by studying Actinobacteria isolated from the Cuatro Cienegas Basin (CCB), an oasis in the Chihuahuan desert, North of Mexico. This site has very little primary productivity because of its ultra-oligotrophy in both phosphorous (below 0.5 micromolar) and iron (in the nanomolar range) (Elser *et al.* 2005). Nevertheless, despite its low-key nutrients, CCB is largely biodiverse as the result of a very cohesive and structured community (Souza *et al.* 2008). Because of the evolution of *Micrococcus* and *Streptomyces* in this unique environment, we anticipate that our evolutionary analyses can assist in defining candidate genes for molecular ecological analyses and further functional characterization in both the laboratory and environmental settings.

MATERIAL AND METHODS

Isolation and identification of bacterial species

Water samples, with nanomolar concentrations of iron (Souza *et al.* unpublished data), from the Churince hydrological system were filtered (0.22 μM). Sediments from shallow areas of the Churince system were collected and homogenized in sterile water. The recovered filters and homogenized sediments were used for isolation of Actinobacteria in serial dilutions on plates with the following media: SFM: 20 gr/L mannitol; 10 gr/L soy flour; 20 gr/L agar in tap water (Kieser *et al.* 2000); CMM: 10 gr/L sucrose; 1.2 gr/L TRIS base; 250 mg/L magnesium sulphate heptahydrate; 5 mg/L lithium chloride; 2 gr/L yeast extract; 1 gr/L

ammonium chloride; 4 gr/L casaminoacids; 15 gr/L agar (Ftayeh, von Tiedemann and Rudolph 2011); and R2NP minus pyruvate: 0.5 gr/L yeast extract; 0.5 gr/L casaminoacids; 0.5 gr/L dextrose; 0.3 gr/L dipotassium phosphate dissolved in 50% sea salt solution (Instant Ocean®, Blacksburg, USA) at pH7 (D'onofrio, Crawford and Stewart 2010). All isolation plates contained 100 μg/mL of cycloheximide to inhibit the growth of fungi, and 50 μg/mL of nalidixic acid to select for Gram-positive bacteria. Isolation of siderophore-producer strains was performed in CMM plates with 2,2'bipyridyl (D216305, Sigma-Aldrich) at a final concentration of 200 μM. After 3 to 7 days of incubation at room temperature, actinomycete-like colonies were re-streaked on the corresponding isolation media until axenic cultures were obtained. Nutrient agar medium (BD Bioxon, Mexico) was used for follow-up characterization experiments.

Strain identification was done through 16S ribosomal RNA gene amplification and sequencing, using F27 (AGAGTTTGATCMTGGCTCAG) and R1492 (TACGGYTACCTTGTTACGACTT) primers. PCR products were sequenced at the Langebio DNA sequencing facilities (Irapuato, Mexico) and manually assembled and edited using Chromas 2.6.2 (http://technelysium.com.au/wp/chromas/). Only the regions of high quality were kept for further analyses (Table S1, Supporting Information). The taxonomic classification of the isolates was done using Blast to search for best hits of the 16S rRNA amplicons of the isolates in the non-redundant database of GenBank. The matching sequences were retrieved for phylogenetic analysis. The sequenced amplicons and the sequences retrieved from GenBank were aligned with MUSCLE v3.8.31 (Edgar 2004), and used for construction of a phylogenetic tree using MrBayes v3.2.3 with a HKY model for a million generations, in two runs of four chains each, enough to converge into a stationary distribution.

Bacterial cultivation under iron-limiting conditions and identification of siderophores

The ability of the isolates for siderophore production was addressed using the Chrome Azurol S (CAS) reagent (Schwyn and Neilands 1987). The isolates were grown as lawns in CMM plates with and without 2,2' bipyridyl, and incubated for 48 h at 30°C. Pieces of agar from grown cultures (Table S1) were placed on top of CAS agar plates, and after 16 h of incubation, the plates were inspected for the presence of orange halos indicating the production of hydroxamate siderophores (Table S1 and Fig. S3, Supporting Information). To analyze the effect of iron limitation upon the bacterial interactions, organisms were grown with and without 2,2'bipyridyl in nutrient agar plates for 48 h. This media was selected because most strains grew well after 48 h of incubation without 2,2' bipyridyl (Fig. S11, Supporting Information). Pieces of agar from the grown cultures were placed on top of lawns of CH1 grown on plates containing 2,2'bipyridyl, and incubated for 24 more hours (Fig. 5). To obtain fermentation extracts for LC-MS analysis, 150 mL liquid cultures in R2NP medium, with and without 2,2' bipyridyl, grown in 500 mL Erlenmeyer flasks were incubated at 30°C for 7 days with agitation at 180 rpm.

Genome sequencing, annotation and mining for iron-metabolic genes

The genomic DNA of selected strains was extracted with standard protocols and sequenced using the MiSeq Illumina platform in the 250 bases paired-end format at the Langebio Genomic Services unit, except for isolate CC77, which was sequenced with the Illumina NextSeq 150 bases paired-end format. The reads obtained were trimmed using Trimmomatic v0.32 (Bolger, Lohse and Usadel 2014) and assembled using Velvetg and Velveth v1.2.10 (Zerbino and Birney 2008). K-mers ranging from 31 to 171 (increasing 10 units per iteration) were tested, and the best assembly was selected for annotation and analysis. Annotation was performed with RAST (Aziz *et al.* 2008) and antiSMASH v3.0 (Weber *et al.* 2015). To further support roles on iron metabolism, for both the predicted siderophore BGCs and SBPs (Table 1), we identified the regulatory sequences of 'iron-boxes' (Tunca *et al.* 2007) by means of exploiting the consensus 'TNANGNNAGGCTNNCCT' sequence as query. These searches were done using the Artemis genome browser v16 (Carver *et al.* 2012). Putative products from BGCs were inferred based on sequence homology to previously reported pathway intermediates.

Phylogenomic analysis of DFO biosynthesis and transport systems

Genomes for the phylogenomics analysis of DFO biosynthesis were selected from a representative taxonomic coverage of Actinobacteria, and retrieved from the GenBank (Table S2, Supporting Information). The amino acid sequences of DesA, DesB, DesC and DesD from *Streptomyces coelicolor* were used as queries for BLASTP searches within the genomes database with E-value cutoff of 1E-12 and bit score cutoff of 200. Genomes containing contiguous *des* homologs were classified as putative DFO producers, and their amino acid sequences were retrieved. This set of sequences was complemented with DesA-D orthologs from other non-Actinobacteria species reported to produce DFOs (Essén, Johnsson and Bylund 2007; Smits and Duffy 2011). These amino acid sequences were aligned with MUSCLE v3.8.31 (Edgar 2004), trimmed and concatenated, and the resulting matrix was used for phylogenetic reconstruction with MrBayes v3.2.3 (Huelsenbeck and Ronquist 2001), with the 'aamodelpr' parameter set to 'mixed' and two runs of four chains each for a million generations, enough to converge into a stationary distribution. The best model with a posterior probability of 1 was found to be WAG. For SBP phylogenetic analysis, the protein sequences of CchF, CdtB and DesE homologs were retrieved from selected genomes using BLASTP with an E-value cutoff of 1E-12 and bit score cutoff of 100. These amino acid sequences were used for phylogenetic reconstruction using MrBayes v3.2.3, as described above.

The genome context of the *des* clusters (Fig. 1) and the SBP-coding genes *cchF, cdtB* and *desE* (Figs S5-S9, Supporting Information) were generated using our own scripts. We searched for DesC homologs with BLASTP with E-value cutoff of 1E-12 and bit score cutoff of 200, and retrieved its gene neighborhood up to 5 Kbp upstream and downstream from the genomes annotated with RAST in GenBank format (Aziz *et al.* 2008). The DesABCD and penicillin amidase DesG homologs within this region were identified and classified as groups of homologs using BLASTP (cutoff e-value of 1E-9).

Identification of siderophores produced by CH1, CH3, CH7 and CC71

Samples were prepared and analyzed as previously reported (Barona-Gómez *et al.* 2004, 2006), with minor modifications. HPLC was carried out using a binary pump (Agilent 1200)

Table 1. Selected genome features of Actinobacteria strains reported in this study.

Strain	Accession number	Genome size (Mbp)	Predicted siderophore BGCs	DesG Homologs	Identified SBP	Detected siderophores
Microbacterium sp. CH1	LOSO00000000	3.55	0	None	Standalone *cdtB* Standalone *cchF*	None
Micrococcus sp. CH3	LOSP00000000	2.68	1	Within the *des* BGC	BGC-*desE* Standalone *cchF*	Aryl-dFO
Micrococcus sp. CH7	LOSQ00000000	2.51	1	Within the *des* BGC	BGC-*desE* Standalone *cchF*	Aryl-dFO
Streptomyces sp. CC71	LOSR00000000	7.89	3	Not found	BGC-*desE* BGC-*cchF* Standalone *cdtB*	dFO-E, dFO-B, Coelichelin
Streptomyces sp. CC77	MKXA00000000	6.81	2	Outside the *des* BGC	BGC-*desE* Standalone *cdtB*	dFO-B, Aryl-dFO, propionyl-dFO
Streptomyces sp. CC53	MKXB00000000	6.98	2	Outside the *des* BGC	BGC-*desE* Standalone *cdtB*	dFO-B, Aryl-dFO, propionyl-dFO

equipped with a diode array detector with a fraction collector, and fitted with a ZORBAX Eclipse XDB-C18 (Agilent, Santa Clara, USA) analytical column (4.6 × 150 mm 5 μm, column temperature 25°C). The mobile phase comprised a binary system of eluent A, 0.1% trifluoroacetic acid, and eluent B, 100% acetonitrile. The run consisted of an isocratic elution of 90% A: 10% B, for 10 min, followed by a gradient of 0:100 over 8 min, 10 min isocratic conditions 0:100, a gradient to 90:10 over 8 min and 10 min to isocratic conditions at 90:10 (A/B). The tris-hydroxamate-$Fe3^{+}$ complexes formed upon addition of iron chloride to the extracts were detected by monitoring absorbance at a wavelength of 435 nm. Selected fractions were collected for analysis in an ion trap LTQ Velos mass spectrometer (Thermo Scientific, Whaltam, USA). MS-MS analysis of selected ions was performed with a collision energy of 20 eV.

RESULTS

Phylogenomic reconstruction of DFO genes

To gain insights into the relationship between DFOs chemical diversity, which we assume here to be related to their cognate biosynthetic routes and transport machineries, and its taxonomic distribution, we reconstructed the evolutionary history of the DFO BGC. For this purpose, we first selected the genomes of 93 species belonging to the phylum Actinobacteria, and defined their taxonomic relationships using a species tree constructed with the sequences of their RNA polymerase beta subunits or RpoB (Fig. S1, Supporting Information). The obtained tree shows overall congruent taxonomic relationships for all strains, other than for *Microbacterium* sp. KROCY2 (accession PRJNA195886), which seems to be a member of the genus *Kocuria*.

We then identified and retrieved the *des* genes found to be conserved throughout the analyzed organisms. Based on previous reports, the DFOs or *des* BGC was assumed to consist of only the *desABCDEF* genes (Barona-Gómez *et al*. 2006). After taking into account the possibility of paralogous genes, we found *des* genes to be present in 69 of the 93 analyzed organisms. Specifically, the *desABCD* genes when present were always conserved within a single locus, whereas the *desEF* genes were linked to the latter genes solely in the genus *Streptomyces* (Table S1). The obtained Des matrix was enriched with the protein products of the orthologous *desABCD* genes from other organisms known to produce dFOs, including species from the Proteobacteria genera *Pseudomonas*, *Erwinia*, *Photorabdus*, *Xenorhabdus* and *Pantoea* (Essén, Johnsson and Bylund 2007; Smits and Duffy 2011). A concatenated DesABCD phylogenetic tree was then constructed and used to project the genomic context surrounding the *desABCD* genes, as well as other related genes present somewhere else in the analyzed genomes (Fig. 1).

To complement our phylogenomics analysis with meaningful environmental isolates related to iron oligotrophy, selective isolation of species belonging to the phylum Actinobacteria was performed from water and sediments of the CCB. To select for potential siderophore producer strains, we used general Actinobacteria selective media supplemented with 2,2'-bipyridyl, an iron quencher that has been shown to serve as a good strategy to mimic iron limitation, and to induce siderophore biosynthesis without added toxicity (Barona-Gómez *et al*. 2006; Tierrafría *et al*. 2011). As a result, we obtained 55 isolates that could grow under iron limitation, all belonging to the phylum Actinobacteria, as revealed by 16S rRNA phylogenetic analysis (Fig. S2, Supporting Information). The obtained isolates were distributed throughout the genera *Arthrobacter* (3), *Brachybacterium* (2), *Brevibacterium* (1), *Citricoccus* (3), *Corynebacterium* (3), *Dietzia* (2), *Kocuria* (8), *Microbacterium* (10), *Micrococcus* (7), *Nocardia* (1) and *Streptomyces* (15) (Table S1).

These isolates were then screened for siderophore production using the low-resolution CAS assay (Fig. S3, Supporting Information), finding positive results only for 16 organisms (Table S1). As expected, *Micrococcus* (two out of four strains) and *Streptomyces* (11 out of 11 strains) were positive for siderophore production on the CAS assay, whereas *Microbacterium* isolates, despite the relative large number of strains obtained under iron-limited conditions, seem incapable of producing siderophores (zero out of five strains), at least under these conditions. Similarly, none of the two *Citrococcus* strains tested for siderophore production, including strain CH26A isolated previously from the CCB, and whose genome includes the *desABCD* genes (Hayano-Kanashiro *et al*. 2011), were positive for the CAS assay under the conditions used. Given that the CAS assay may potentially give false negatives, as emphasized by the case of *Citrococcus* CH26A that contains the *des* genes, we randomly selected three CAS-negative strains and checked for their ability to produce DFOs

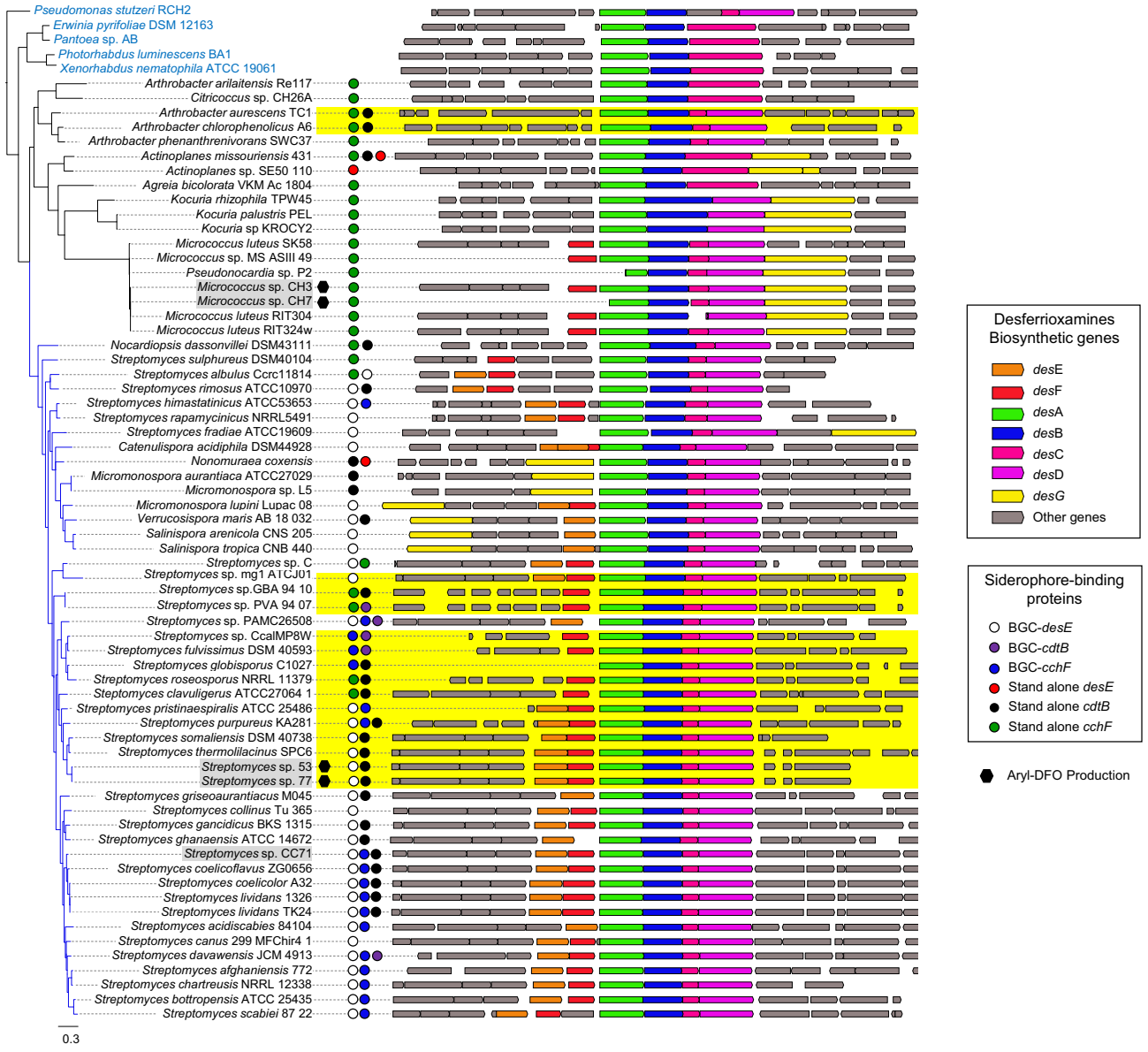

Figure 1. Evolution of the desferrioxamine biosynthetic gene clusters (Des) and siderophore transporters. The phylogenetic tree was constructed with a concatenated matrix of DesABCD orthologs. Highlighted taxa correspond to CCB isolates and blue branches indicate myceliated species. The tree outgroup includes Gram-negative strains, which acquired the *des* BGC, and they are shown in blue. Occurrence of SBP homologs is shown with colored circles. The gene context of the *desABCD* locus for each taxon is shown on the right-hand side. The *desG* genes are shown as yellow arrows when found within the *des* BGC, and highlighted by yellow boxes when *desG* is located elsewhere in the genome, but under the control of an iron box.

under the iron-limited conditions used for original isolation, by means of HPLC profiling (see also next subsection). As expected, neither the *Dietzia* strain CH61, the *Corynebacterium* strain CH63 or the *Microbacterium* strain CH1, which were analyzed, showed signs of siderophore production (Fig. S4, Supporting Information).

On the basis of these results, we selected six isolates belonging to the genera *Microbacterium* (1), *Micrococcus* (2) and *Streptomyces* (3) for further genomic analysis. After 16S rRNA analysis, strain CH1 was linked to *Microbacterium paraoxydans* (water); strains CH3 (water) and CH7 (sediment) were linked to *Micrococcus luteus*; and strain CC71 and strains CC53/CC77 (all from sediment) were related to *Streptomyces rochei* and *S. rubrolavendulae* MJM4426, respectively (Fig. 1). CH1 was selected as a reference of an organism unable to produce siderophores, whereas the remaining strains are organisms from different taxa able to produce siderophores (as shown by CAS assay, also see HPLC metabolite profiling, following section).

The genomes of the aforementioned organisms were sequenced, assembled and thoroughly annotated. In addition to general functional annotation using RAST (Aziz *et al.* 2008) and antiSMASH (Weber *et al.* 2015) for natural products BGCs, conserved DNA motifs corresponding to iron boxes, known to be involved in iron regulation in these bacteria (Tunca *et al.* 2007, 2009), were used to implicate the predicted BGCs with iron metabolism. This combined strategy revealed that the genomes of strains CH3, CH7, CC53, CC71 and CC77 include the *des* BGC, and that the *cch* BGC is only present in CC77. Moreover, the genomes of these organisms include at least one extra transport system to the one associated with the *des* and *cch* BGCs. In

contrast, the genome of strain CH1 lacks any sign of a siderophore-like BGC, but contains iron boxes upstream of at least two siderophore transport systems (Table 1). Thus, our genomic analysis for CH1 is in agreement with the inability of this strain to produce siderophores, while the identification of iron transporters implies dependency on siderophores produced by other organisms. Based on these results, we incorporated these organisms to our phylogenomics to search for specific evolutionary patterns, and perform experimental characterization as described further.

Evolutionary patterns of DFO biosynthesis

Analysis of the DesABCD concatenated phylogenetic tree shown in Fig. 1 reveals gene fusions between DesC, an acyl CoA-dependent acyl transferase, and DesD, the canonical NRPS-independent peptide synthetase, in both non-Actinobacteria and Actinobacteria; and between DesB, a FAD-dependent amine monooxygenase, and DesC, solely in the actinobacterial organisms *Kocuria rhizophila* TPW45, *K. palustris* and *Microbacterium* KROCY2, which seems to be actually a *Kocuria* species as previously discussed. These fusions may have a bearing on the iterative assembly of the formation of amide bonds catalyzed by DesD (Barona-Gómez *et al*. 2004; Telfer *et al*. 2016), leading to different DFOs molecular scaffolds. Alternatively, this could also be the result of selective pressure to couple the transcription of these two genes for non-enzymatic reasons. In contrast, no fusions involving DesA, a pyridoxal 5-phosphate-dependent descarboxylase, could be detected, probably due to mechanistic restrictions, regulation of the pathway or the metabolic commitment of lysine as precursor, as previously suggested (Burrell *et al*. 2012).

Figure 1 also shows that the *des* BGC present in the *Micrococcus* strains analyzed, in addition to having the *desABCD* operon, includes a previously unnoticed conserved gene. This gene (colored in yellow in Fig. 1) is annotated as a penicillin amidase, an enzyme responsible for the reversible addition of an aryl group to a primary amine. The proximity, conservation and functional annotation of this *Micrococcus* gene, termed here *desG*, strongly suggest a functional association of this gene with DFOs biosynthesis. Moreover, after performing homology searches using *desG* from CH3 as query sequence, coupled with analysis based in the iron-box motif, we found *desG* orthologs outside the *des* BGC but next to an iron box (highlighted with a yellow box in Fig. 1), in species belonging to the genera *Arthrobacter* and *Streptomyces*, including strain CC77 (Table 1 and Fig. 1). Based on the observation that expression of DesG orthologs outside the *des* BGS may be regulated via an iron box, we hypothesized that DesG is involved in chemical diversification of DFOs.

In the case of the strains belonging to the genus *Micrococcus*, this proposal is in agreement with a previous report of the production of arylated-DFOs by *Micrococcus* species (D'onofrio, Crawford and Stewart 2010). Therefore, we propose that DesG is responsible for the synthesis of aryl-substituted hydroxamic acids via acylation of either monomers or dimers of *N*-hydroxycadaverine, as shown in Fig. 2. Moreover, according to our phylogenomic analysis, this pathway may exist in at least two subclades with a common DesABCD phylogenetic signal, which includes the aquatic strains CC53 and CC77. Interestingly, this clade includes other taxonomically distantly related aquatic organisms, such as *Verrucosispora maris*, *Salinispora tropica* and *Sa. arenicola*, in addition to isolates CH3 and CH7.

Evolutionary patterns of hydroxamate-specific SBP-coding genes

To gain insights into the role of putative DFO transporters from a phylogenomics perspective, we investigated the occurrence and genome context of SBP-coding genes throughout the 69 genomes analyzed in Fig. 1. This dataset was complemented with the genomes of *Microbacterium* CH1 (this study) and *Amycolatopsis* sp. AA4 (Traxler *et al*. 2012), which are expected to be capable of utilizing DFOs despite the fact that they lack a *des* BGC. We did this by searching for homologs of the *cchF*, *cdtB* and *desE* genes, and implicating them with iron metabolism by confirming the presence of a consensus iron box next to them. We found that most analyzed organisms in our dataset have larger siderophore acquisition capabilities than those directly linked to DFOs (Fig. 1). Thus, we analyzed SBPs from a phylogenetic perspective and used their genome context to associate them to different biosynthetic contexts (Fig. 3). The evolutionary patterns that were revealed after this analysis are described in detail in the following paragraphs.

The *desE* homologs are only present in myceliated Actinobacteria that undergo morphological differentiation, either associated with the *des* BGC, termed 'BGC-*desE*'; or independently of any BGC, termed 'stand-alone *desE*' (Fig. S5, Supporting Information). For the latter case, we also noticed that *desE* is often part of an operon that includes genes encoding for the permease and ATPase components needed to complete a functional siderophore transport system, which is not the case for BGC-*desE* that lacks those genes (Fig. 1), as originally noticed (Barona-Gómez *et al*. 2006). These observations may be related to previous observations implicating *desE* in morphological development of *S. coelicolor* and *Amycolatopsis* sp. AA4 (Tierrafría *et al*. 2011; Traxler *et al*. 2012). Indeed, a stand-alone *desE* homolog upstream an iron-box promoter element is present in the genome of the latter organism, which may provide an alternative transport system to the one encoded in the amychelin BGC.

The *cchF* homologs previously associated with the *cch* BGC, termed 'BGC-*cchF*', are only present in members of the genus *Streptomyces* (Fig. S6, Supporting Information). In contrast, other *cchF* homologs not linked to a *cch* BGC, termed 'stand-alone *cchF*', are present in many organisms belonging to distantly related genera, such as *Streptomyces, Arthrobacter*, *Citricoccus*, *Actinoplanes*, *Agreia, Kocuria*, *Pseudonocardia, Clavibacter, Nocardiopsis*, *Micrococcus* and *Microbacterium* (Fig. S7, Supporting Information). This type of stand-alone SBP-coding gene is also present in our environmental strains CH1, CH3 and CH7. Interestingly, when a BGC-*cchF* SBP is present, a second unrelated SBP-coding gene is always present, whereas the stand-alone *cchF* is often found irrespective of any other siderophore biosynthetic or transport systems (Figs 1 and 3).

The *cdtB* homolog, termed here 'stand-alone *cdtB*' and previously described as a BGC-independent gene in *S. coelicolor* (Bunet *et al*. 2006; Tierrafría *et al*. 2011), is broadly distributed throughout the analyzed genomes (Fig. S8, Supporting Information). However, in *S. davawensis* JCM 4913, *Streptomyces* sp. CcalMP8W, *Streptomyces* sp. PAMC26508, *Streptomyces* sp. PVA 94 07 and *S. fulvissimus* DSM 40 593, *cdtB* homologs are present just upstream of genes coding for peptide synthetases that seem to be part of BGCs, and thus we call them 'BGC-*cdtB*' (Fig. S9, Supporting Information). Interestingly, in *S. fulvissimus*, based on our own annotation, the corresponding synthetase seems likely to be responsible for the production of valinomycin (Myronovskyi *et al*. 2013), a depsipeptide ionophore that has not been previously linked to iron metabolism.

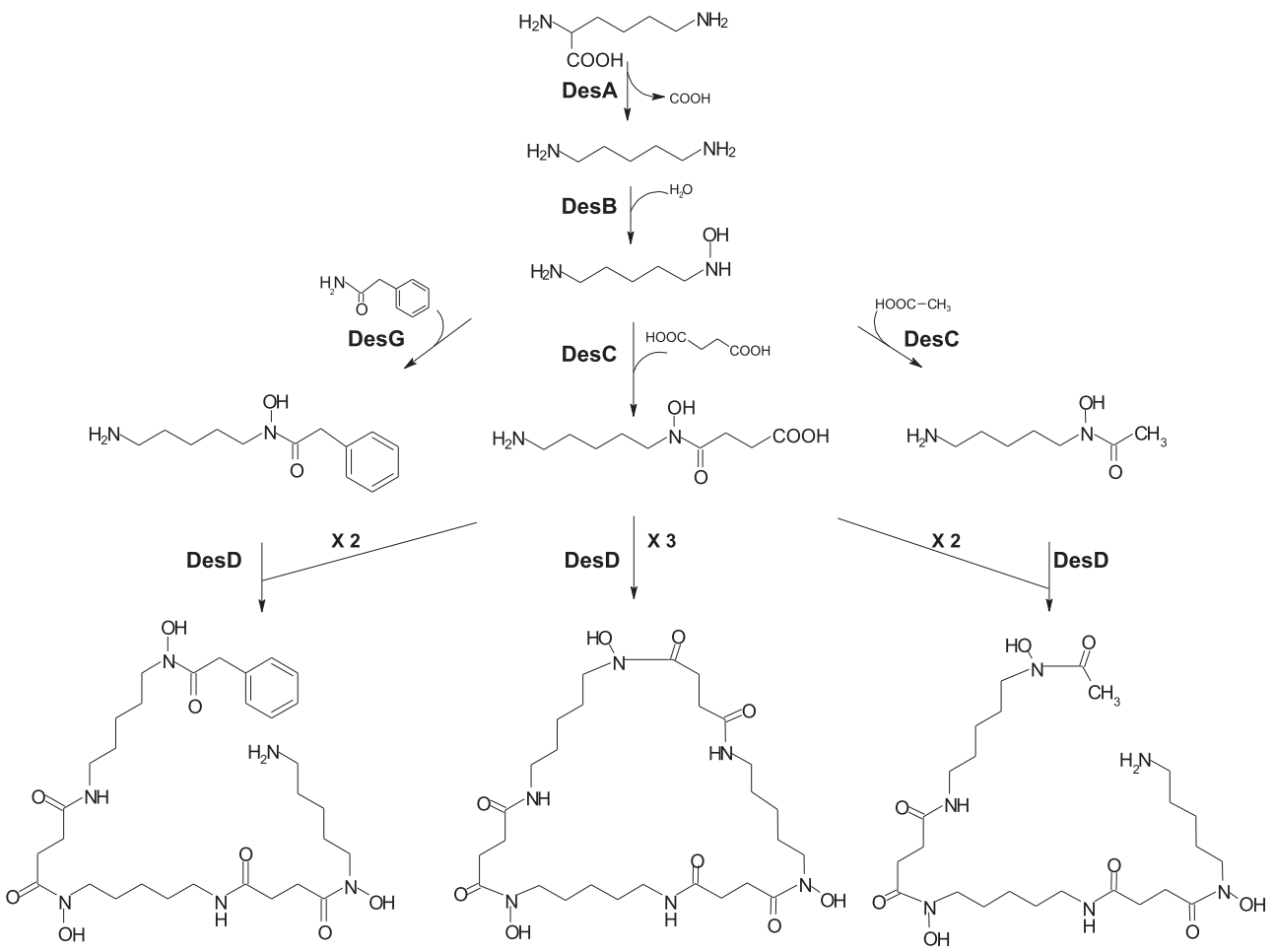

Figure 2. Biosynthetic logic of desferrioxamines including the proposal for the incorporation of phenylacetate by DesG, a homolog of the penicillin amidase, to produce aryl-desferrioxamines.

The aforementioned evolutionary patterns can be summarized as follows: (i) all SBP subfamilies include both BGC-associated and stand-alone SBPs; (ii) all BGC-*desE* homologs are never associated with ATPase or permease components needed for a complete ABC transport system, which contrasts with stand-alone *desE* scenarios; (iii) the BGC-*cdtB* homologs seem to be recently recruited and may have a functional connection with the products of their cognate BGCs, but not necessarily via their transport. This latter observation is supported by the fact that these homologs are either associated to a valinomycin BGC, an ionophore not know to transport iron, to a complete coelichelin BGC that includes its own *cchF* homolog, or to an unknown non-ribosomal peptide synthetase system not related to any known siderophore; and (iv) the *cchF* homologs evolved more recently and are always associated with the ATPase and permease components of the ABC transporter system.

Taken together, these patterns suggest that bacterial SBPs evolved from a generalist ancestor devoted to iron acquisition, which seems closer to *cdtB*. Such ancestor must have been able to transport a wide range of siderophores, whilst unrelated to their biosynthesis. Divergence of SBPs occurred later with the appearance of *desE*, only in myceliated species, and *cchF* in a broader range of actinomycetes. Both subfamilies were recruited into DFO and coelichelin BGCs, respectively. Remarkably, despite broad distribution of *cchF*, only myceliated species include *cchF* homologs that are linked to the *cch* BGC. In the case of *desE*, its recruitment came along with detachment from ATPase and permease components from the ABC transport system. In other words, coelichelin production may have led to the loss of Des-specialized ATPase and permease components for DFOs, specifically in organisms that undergo developmental differentiation, as further discussed.

Profiling of hydroxamate-type siderophore production

In order to establish links between the predicted *desG*-related biosynthetic pathway and its products, we aimed to detect siderophores that were produced by CCB strains. For this purpose, we cultivated CH1, CH3, CH7, CC53, CC71 and CC77 on iron-limiting conditions, and analyzed the soluble extracts of the supernatant. Iron chloride was added to the extracts before HPLC analysis, to specifically detect fractions containing iron complexes at a wavelength of 435 nm (Fig. 4). This strategy is useful to distinguish siderophores from metabolites that might absorb at this wavelength irrespective of iron. Moreover, HPLC fractions containing iron chelates were collected and analyzed using MS/MS (Fig. S10, Supporting Information). These experiments showed that CC71 produces coelichelin (*m/z*, 619.26), ferrioxamine B (*m/z*, 614.26) and ferrioxamine E (*m/z*, 654.26); that CC53 and CC77 produced ferrioxamines B, E and two

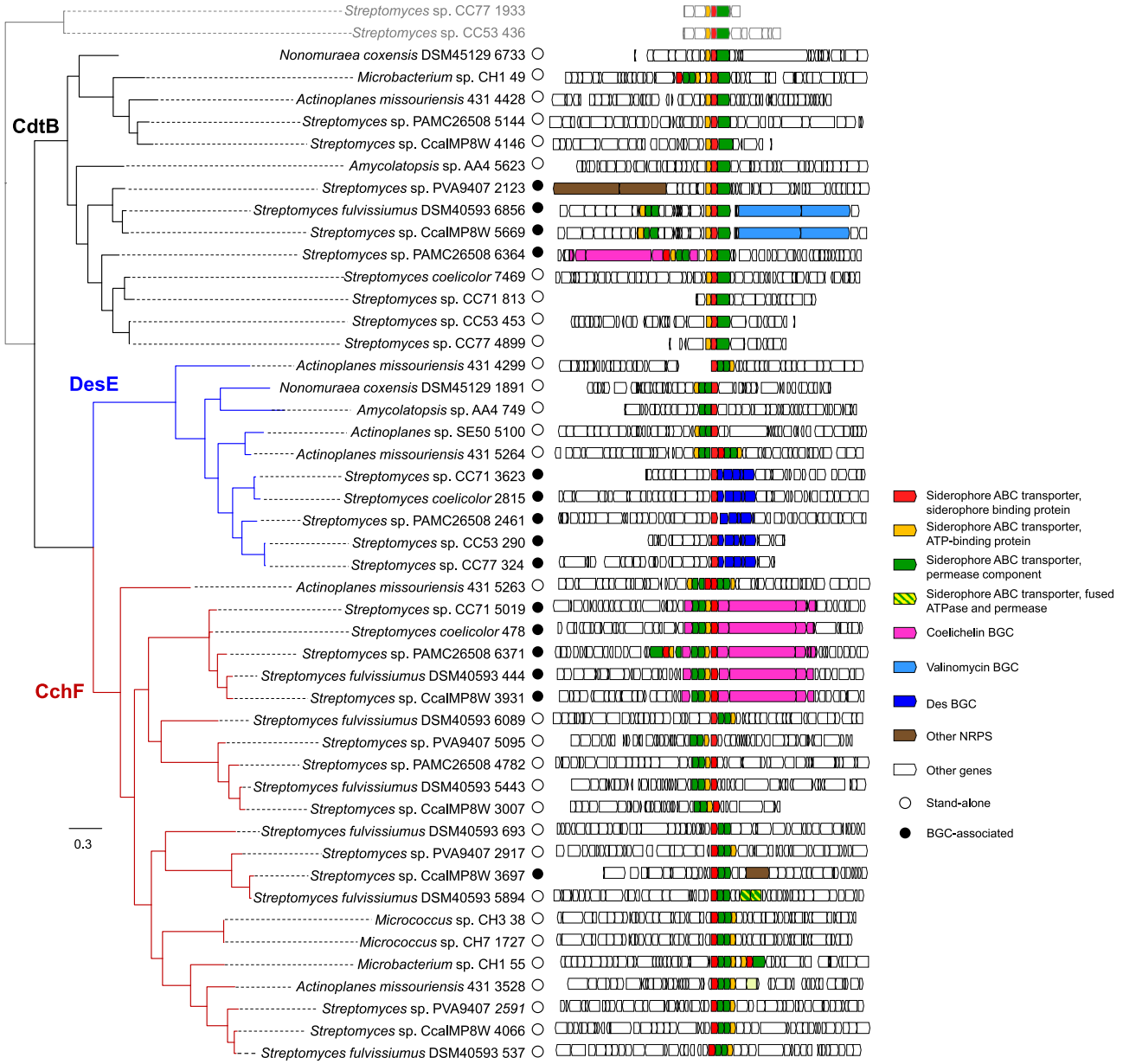

Figure 3. Evolution of the SBPs. The phylogenetic tree was constructed with a matrix of CdtB, DesE and CchF orthologs. All homologs, except 1943 and 436 from CC77 and CC53, used as outgroups, are associated with at least one iron box. The association of SBPs with specific BGCs is represented with circles. The gene context for each taxon is shown on the right-hand side. The branches related for each subfamily are colored: black for CdtB, blue for DesE and red for CchF.

unusual variants, a propionyl-substituted ferrioxamine (propionyl-ferrioxamine, m/z = 628.17) and a phenylacetyl substituted variant (aryl-ferrioxamine, m/z, 690.26); and CH3 and CH7 produced the aryl-ferrioxamines. In contrast, none of the known siderophores could be detected in extracts of CH1 (Fig. 4), nor in the control strains CH63 and CH61 used in previous section for validation of our screening approach.

The identification of acyl-ferrioxamine 1 in CH3 and CH7, two strains that are taxonomically related to *M. luteus*, agrees with previous reports on the production of the same molecule by environmental isolates linked to the same species (D'onofrio, Crawford and Stewart 2010). However, to our knowledge, this is the first report of aryl and propionyl ferrioxamines in species belonging to the genus *Streptomyces*.

Siderophore-mediated growth stimulation in co-cultures

In agreement with the genomic data, growth of CH1 was severely compromised when cultivated under iron-limited conditions in both liquid and solid media, whilst a detrimental effect was observed on the remaining strains. This observation supports the hypothesis that CH1 depends on siderophores produced by other strains sharing the same ecological niche. Therefore, to confirm the ability of CH1 to acquire siderophores from other species, we cultivated lawns of CC71, CH1, CH3 and CH7 in iron-limited conditions. As expected, growth could be observed after 48 h of incubation in all plates, except in those plates containing CH1 (Fig. S11, Supporting Information). Plugs of agar from

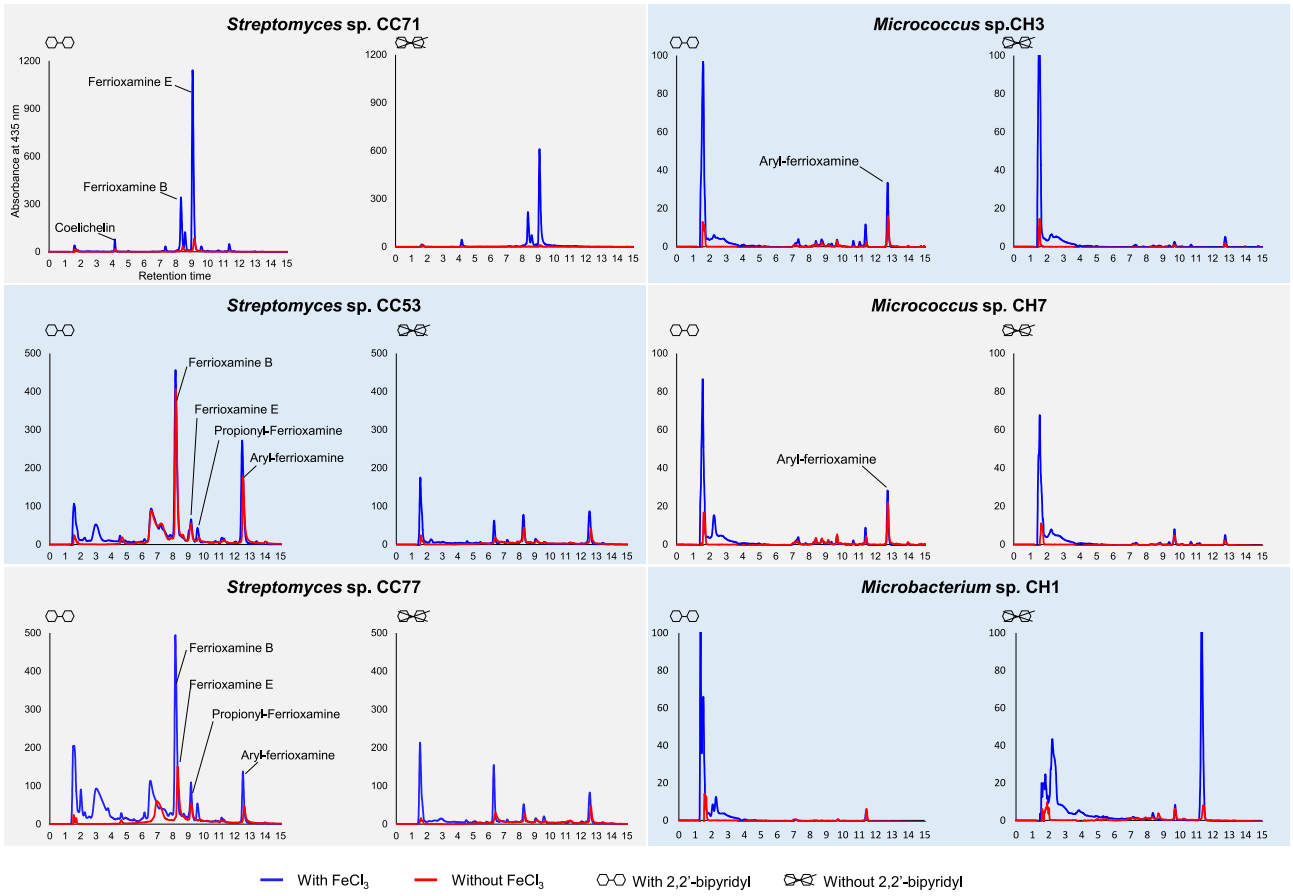

Figure 4. Siderophore profiling of CCB isolates. Labeled peaks were collected and analyzed using MS/MS. The *x* axis shows retention time in minutes and the *y* axis shows absorbance units at 435 nm. Blue traces correspond to samples where $FeCl_3$ was added and red traces to samples without iron. Peaks related to siderophores are considerably larger on samples obtained under iron limitation (with 2,2'-bipyridyl), and their absorbance increases upon addition of iron.

the iron-limited plates with growing lawns of CC71, CH3 and CH7, and from the plate without 2,2'-bipyridyl where CH1 could grew, were placed on top of lawns of CH1 grown in nutrient agar (Fig. 5A). This experiment shows that growth of CH1 is promoted by siderophores from cultures of CH3, CH7 and CC71 grown under iron-limited conditions. In fact, further experiments with purified DFOs (Fig. 5B) confirmed the ability of CH1 to use iron from ferri-xenosiderophores produced by other microorganisms sharing the same ecological niche and its dependence on them to survive.

DISCUSSION

We have performed an evolutionary study of DFO biosynthesis and siderophore transport using a genomic database enriched with non-model organisms isolated from the CCB, an aquatic system extremely limited in phosphorous and iron. The conservation of the des cluster in *Streptomyces*, and its distribution in few Actinobacteria genera, suggests that the cluster originated in an early-diverging actinobacterial lineage. This BGC then radiate with the speciation of the genus *Streptomyces*, with some more distant horizontal gene transfer events involving Gram-negative bacteria (Essén, Johnsson and Bylund 2007; Smits and Duffy 2011).

An important observation derived from the integration of the Des phylogenomic analysis and siderophore production profiles from CCB strains is the finding of DesG. LC-MS data demonstrated that CCB strains CH3, CH7, CC53 and CC77, which have a *desG* homolog either as part of the *des* BGC or independently elsewhere in the chromosome, produce Aryl-DFOs. We postulate that DesG synthesizes these specialized metabolites via incorporation of phenyl-acetate. While our biosynthetic proposal remains to be experimentally validated, it is in agreement with the fact that no aryl-substituted DFOs have been reported in *Streptomyces coelicolor*, which lacks a *desG* homolog. Instead, aliphatic acyl chains have been found as substituents in this organism, specifically as a response to the siderophore-pirating strain *Amycolaptosis* sp. AA4 (Traxler *et al.* 2013), or after cultivation at 37°C, which is a stressful condition for this model organism (Sidebottom *et al.* 2013).

Interestingly, acylation has been shown to be a common structural modification of marine DFOs, such as those produced by members of the genus *Salinispora* (Ejje *et al.* 2013). However, despite the fact that our phylogenomic analyses shows the presence of *desG* homologs in two *Salinispora* genomes, to our knowledge, production of aryl-substituted DFOs has not been reported in this group of organisms. A possible interpretation of the ability of aquatic actinomycetes to synthesize hydrophobic DFOs could be that incorporation of acyl or aryl groups provides a strategy to control its solubility, when competition for iron chelate complexes is on place. In this scenario, acylated DFOs will stay closer to the producer strain allowing for iron chelation in its proximity, thus facilitating intake. Such a mechanism would be evidently advantageous in a series of other

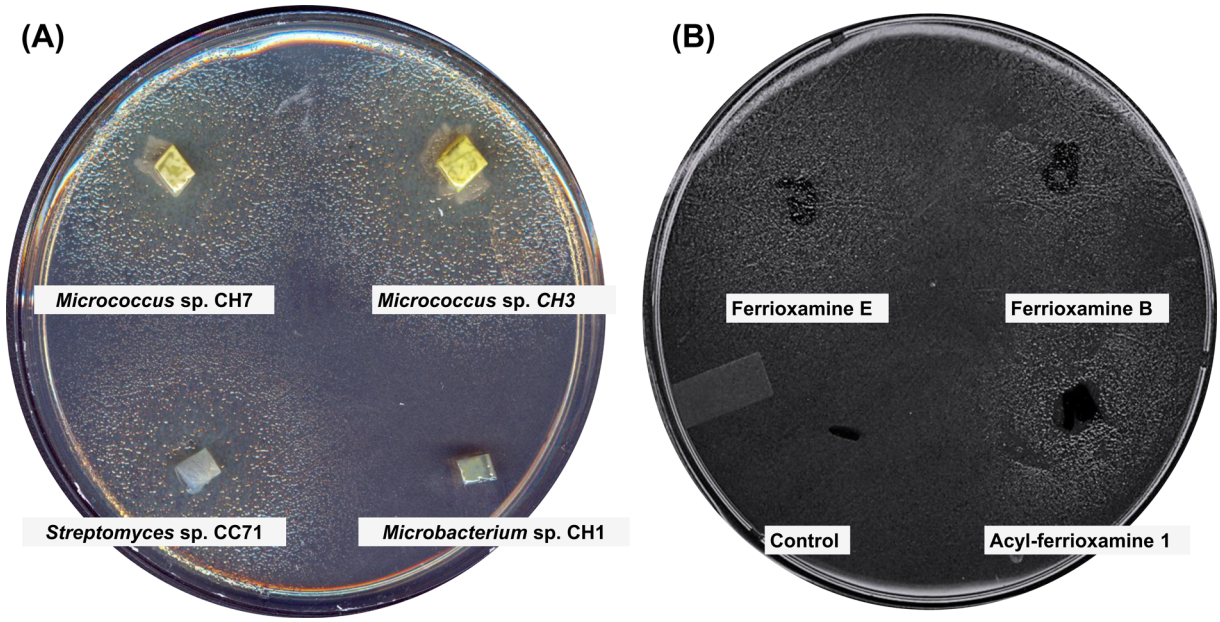

Figure 5. Siderophore-acquisition profiling of CCB strains. **(A)** Effect of iron limitation on interactions between CH1 plated as a lawn and predicted not to produce siderophores, and other siderophore producer strains. CH1 grows better around pieces of agar with siderophore producer strains. **(B)** Acquisition of specific ferrioxamines by CH1. The non-producer strain is able to grow in the areas where ferrioxamines E, B and acylferrioxamine 1 were added, and water was used as control.

scenarios, including biofilm formation and in water-filled pores of soil-dwelling filamentous organisms.

Synthesis of the evolutionary patterns found for CchF, CdtB and DesE, lead us to propose a model for diversification of SBPs that links DFOs structural diversity with the wealth of SBPs. Our proposal takes into account multifunctionality, namely iron acquisition plus developmental signaling (Tierrafría *et al.* 2011, Traxler *et al.* 2012), as well as multispecificity. Specifically, we propose that bacterial SBPs evolved from a generalist ancestor devoted to iron acquisition able to transport a wide range of siderophores, irrespective of their synthesis that could occurred abiotically or as metabolic side products of promordial bacteria. Such ancestral SBP would resemble DesE, which is still a generalist (Barona-Gomez *et al.* 2006; Bunet *et al.* 2006; Patel, Song and Challis 2010; Tierrafría *et al.* 2011; Arias *et al.* 2015), and may have given place to both specialized transporters associated with specific BGCs. This pattern is in agreement with the fact that the product of the BGC-*cchF* is specific for coelichelin (Patel, Song and Challis 2010), whereas the stand-alone *cchH* versions may have broad siderophore specificity, supporting cooperative or cheating behavior (D'onofrio, Crawford and Stewart 2010). Indeed, strain CH1 provides an example of how an organism could adapt to the ultraoligotrophic environment of CCB following the proposed model.

Given the association of nutritional stress with developmental differentiation in myceliated Actinobacteria, and the exclusive occurrence of DesE homologs on these groups of bacteria, we speculate that the DesE receptors evolved to sense iron scavengers as morphogens, such as DFO-E, while conserving their ability to bind different hydroxamate siderophores, thus becoming multifunctional. The latter scenario implies an adaptive conflict (Des Marais and Rausher 2008), as a transport mechanism that evolved for iron acquisition is co-opted for developmental signaling in organisms that undergo morphological differentiation. In this scenario, appearance of other co-occurring siderophores in myceliated Actinobacteria (Challis and Hopwood 2003), such as coelichelin associated with the specialized SBP CchF, may have occurred as an evolutionary mechanism to deal with this adaptive conflict. Indeed, it has been shown that in *S. coelicolor* coelichelin is the dominant siderophore produced for iron acquisition (Traxler *et al.* 2012). Thus, rather than contingency, as previously proposed (Challis and Hopwood 2003), we provide an evolutionary framework driven by adaptive conflicts that reconcile specialization, multifunctionality and multispecificity.

SUPPLEMENTARY DATA

Supplementary data are available at *FEMSEC* online.

ACKNOWLEDGEMENTS

We thank Yolanda Rodriguez and Alicia Chagolla from the LC-MS unit at Unidad Irapuato Cinvestav-IPN, Guadalupe Mireles and Beatriz Jiménez from the Genomics Services at Langebio, and Araceli Fernandez from the Langebio IT Services, for technical support. Sandra Pérez, Lorena Rodríguez, José Luis Steffani and Mariana Vallejo are gratefully acknowledged for their support during fieldwork, computational analysis and managing the FBG strain collection. We also thank Sébastien Rigali for his useful criticism, which helped us to improve this manuscript.

FUNDING

This work was funded by Alianza World Wildlife Foundation-Fundacion Carlos Slim to Valeria Souza-Saldivar. Laboratorio Nacional de Genomica para la Biodiversidad (Langebio) postdoctoral fellowship to Pablo Cruz-Morales. Scholarships from Consejo Nacional de Ciencia y Tecnologia (Conacyt) de Mexico to Nelly Selem-Mojica and Paulina Mejia-Ponce, and Conacyt postdoctoral fellowship to Cuauhtémoc Licona-Cassani. The work at Francisco Barona-Gomez laboratory is funded by Conacyt grants 179290 and 177568.

Conflict of interest. None declared.

REFERENCES

Arias AA, Lambert S, Martinet L *et al.* Growth of desferrioxamine-deficient *Streptomyces* mutants through xenosiderophore piracy of airborne fungal contaminations. *FEMS Microbiol Ecol* 2015;**91**: fiv080.

Aziz RK, Bartels D, Best AA *et al.* The RAST Server: Rapid Annotations using Subsystems Technology. *BMC Genomics* 2008; **9**:75.

Barona-Gómez F, Lautru S, Francou FX *et al.* Multiple biosynthetic and uptake systems mediate siderophore-dependent iron acquisition in *Streptomyces coelicolor* A3(2) and *Streptomyces ambofaciens* ATCC 23877. *Microbiology* 2006;**152**(Pt 11):3355–66.

Barona-Gómez F, Wong U, Giannakopulos AE *et al.* Identification of a cluster of genes that directs desferrioxamine biosynthesis in *Streptomyces coelicolor* M145. *J Am Chem Soc* 2004;**126**:16282–3.

Bolger AM, Lohse M, Usadel B. Trimmomatic: a flexible trimmer for Illumina sequence data. *Bioinformatics* 2014;**30**:2114–20.

Bunet R, Brock A, Rexer HU *et al.* Identification of genes involved in siderophore transport in *Streptomyces coelicolor* A3(2). *FEMS Microbiol Lett* 2006;**262**:57–64.

Burrell M, Hanfrey CC, Kinch LN *et al.* Evolution of a novel lysine decarboxylase in siderophore biosynthesis. *Mol Microbiol* 2012;**86**:485–99.

Carver T, Harris SR, Berriman M *et al.* Artemis: an integrated platform for visualization and analysis of high-throughput sequence-based experimental data. *Bioinformatics* 2012;**28**:464–9.

Challis GL, Hopwood DA. Synergy and contingency as driving forces for the evolution of multiple secondary metabolite production by *Streptomyces* species. *P Natl Acad Sci USA* 2003;**100**(Suppl 2):14555–61

Craig M, Lambert S, Jourdan *et al.* Unsuspected control of siderophore production by N-acetylglucosamine in streptomycetes. *Environ Microbiol Rep* 2012;**4**:512–21.

Des Marais DL, Rausher MD. Escape from adaptive conflict after duplication in an anthocyanin pathway gene. *Nature* 2008;**454**:762–5.

D'onofrio A, Crawford JM, Stewart EJ. Siderophores from neighboring organisms promote the growth of uncultured bacteria. *Chem Biol* 2010;**17**:254–64.

Edgar RC. MUSCLE: a multiple sequence alignment method with reduced time and space complexity. *BMC Bioinformatics* 2004;**5**:113.

Essén SA, Johnsson A, Bylund. Siderophore production by *Pseudomonas stutzeri* under aerobic and anaerobic conditions. *Appl Environ Microb* 2007;**73**:5857–64.

Elser JJ, Schampel JH, Garcia-Pichel F *et al.* Effects of phosphorus enrichment and grazing snails on modern stromatolitic microbial communities. *Freshwater Biol* 2005;**50**: 1808–25.

Ejje N, Soe CZ, Gu J *et al.* The variable hydroxamic acid siderophore metabolome of the marine actinomycete *Salinispora tropica* CNB-440. *Metallomics* 2013;**5**:1519–28.

Ftayeh RM, von Tiedemann A, Rudolph KW. A new selective medium for isolation of *Clavibacter michiganensis* subsp. *michiganensis* from tomato plants and seed. *Phytopathology* 2011;**101**:1355–64.

Galet J, Deveau A, Hôtel L *et al.* *Pseudomonas fluorescens* pirates both ferrioxamine and ferricoelichelin siderophores from *Streptomyces ambofaciens*. *Appl Environ Microb* 2015;**81**:3132–41.

Hayano-Kanashiro C, López-Arredondo DL, Cruz-Morales P *et al.* First draft genome sequence of a strain from the genus *Citricoccus*. *J Bacteriol* 2011;**193**:6092–3.

Hider RC, Kong X. Chemistry and biology of siderophores. *Nat Prod Rep* 2010;**27**:637–57.

Huelsenbeck JP, Ronquist F. MRBAYES: Bayesian inference of phylogenetic trees. *Bioinformatics* 2001;**17**:754–5.

Kieser T, Bibb MJ, Buttner MJ *et al.* *Practical Streptomyces Genetics*. Norwich UK: The John Innes Foundation, 2000.

Lautru S, Deeth RJ, Bailey LM *et al.* Discovery of a new peptide natural product by *Streptomyces coelicolor* genome mining. *Nat Chem Biol* 2005;**1**:265–9.

Lambert S, Traxler MF, Craig M *et al.* Altered desferrioxamine-mediated iron utilization is a common trait of bald mutants of *Streptomyces coelicolor*. *Metallomics* 2014;**6**:1390–9.

Lewis K, Epstein S, D'Onofrio A *et al.* Uncultured microorganisms as a source of secondary metabolites. *J Antibiot* 2010;**63**: 468–76.

Myronovskyi M, Tokovenko B, Manderscheid N *et al.* Complete genome sequence of *Streptomyces fulvissimus*. *J Biotechnol* 2013;**168**:117–8.

Patel P, Song L, Challis GL. Distinct extracytoplasmic siderophore binding proteins recognize ferrioxamines and ferricoelichelin in *Streptomyces coelicolor* A3(2). *Biochemistry* 2010;**49**:8033–42.

Schwyn B, Neilands JB. Universal chemical assay for the detection and determination of siderophores. *Anal Biochem* 1987;**160**:47–56.

Sidebottom AM, Johnson AR, Karty JA *et al.* Integrated metabolomics approach facilitates discovery of an unpredicted natural product suite from *Streptomyces coelicolor* M145. *ACS Chem Biol* 2013;**8**:2009–16

Sheftel AD, Mason AB, Ponka P. The long history of iron in the universe and in health and disease. *Biochim Biophys Acta* 2012;**1820**:161–87.

Smits TH, Duffy B. Genomics of iron acquisition in the plant pathogen *Erwinia amylovora* insights in the biosynthetic pathway of the siderophore desferrioxamine E. *Arch Microbiol* 2011;**193**:693–9.

Souza V, Eguiarte LE, Siefert J *et al.* Microbial endemism:does phosphorus limitation enhance speciation? *Nat Rev Microbiol* 2008;**6**:559–64.

Telfer TJ, Gotsbacher MP, Soe CZ *et al.* Mixing up the pieces of the desferrioxamine B Jigsaw defines the biosynthetic sequence catalyzed by DesD. *ACS Chem Biol* 2016;**11**: 1452–62.

Tierrafría VH, Ramos-Aboites HE, Gosset G *et al.* Disruption of the siderophore-binding desE receptor gene in *Streptomyces coelicolor* A3(2) results in impaired growth in spite of multiple iron–siderophore transport systems. *Microbiol Biotechnol* 2011;**4**:275–85.

Traxler MF, Seyedsayamdost MR, Clardy J *et al.* Interspecies modulation of bacterial development through iron competition and siderophore piracy. *Mol Microbiol* 2012;**86**:628–44.

Traxler MF, Watrous JD, Alexandrov T *et al.* Interspecies interactions stimulate diversification of the *Streptomyces coelicolor* secreted metabolome. *MBio* 2013;**20**;4.

Tunca S, Barreiro C, Coque JJ *et al.* Two overlapping antiparallel genes encoding the iron regulator DmdR1 and the Adm proteins control siderophore and antibiotic biosynthesis in *Streptomyces coelicolor* A3(2). *FEBS J* 2009;**276**: 4814–27.

Tunca S, Barreiro C, Sola-Landa A *et al.* Transcriptional regulation of the desferrioxamine gene cluster of *Streptomyces coelicolor*

is mediated by binding of DmdR1 to an iron box in the promoter of the desA gene. *FEBS J* 2007;**274**:1110–22.

Wang W, Qiu Z, Tan H *et al*. Siderophore production by actinobacteria. *Biometals*. 2014;**27**:623–31.

Weber T, Blin K, Duddela S *et al*. antiSMASH 3.0-a comprehensive resource for the genome mining of biosynthetic gene clusters. *Nucleic Acids Res* 2015;**43**:W237–43.

Yamanaka K, Oikawa H, Ogawa HO *et al*. Desferrioxamine E produced by *Streptomyces griseus* stimulates growth and development of *Streptomyces tanashiensis*. *Microbiology* 2005;**151**(Pt 9):2899–905.

Zerbino DR, Birney E. Velvet: algorithms for de novo short read assembly using de Bruijn graphs. *Genome Res* 2008;**18**:821–9.